AIP | Applied Physics Letters

Magnetostatic interaction in soft magnetic bilayer ribbons unambiguously identified by first-order reversal curve analysis

M. Rivas, J. C. Martínez-García, I. Škorvánek, J. Marcin, P. Švec, and P. Gorria

Citation: Applied Physics Letters **107**, 132403 (2015); doi: 10.1063/1.4932066
View online: http://dx.doi.org/10.1063/1.4932066
View Table of Contents: http://scitation.aip.org/content/aip/journal/apl/107/13?ver=pdfcov
Published by the AIP Publishing

Magnetostatic interaction in soft magnetic bilayer ribbons unambiguously identified by first-order reversal curve analysis

M. Rivas,[1,a)] J. C. Martínez-García,[1] I. Škorvánek,[2] J. Marcin,[2] P. Švec,[3] and P. Gorria[1]
[1]*IUTA and Departamento de Física, Universidad de Oviedo, Campus de Viesques, 33203 Gijón, Spain*
[2]*Institute of Experimental Physics, Slovak Academy of Sciences, Watsonova 47, 040 01 Kosice, Slovakia*
[3]*Institute of Physics, Slovak Academy of Sciences, Dúbravská cesta 9, 845 11 Bratislava, Slovakia*

(Received 17 April 2015; accepted 18 September 2015; published online 29 September 2015)

Monolithic amorphous $Fe_{73.5}Nb_3Si_{13.5}B_9Cu_1/Fe_{74.5}Nb_3Si_{13.5}B_9$ bilayer ribbons were obtained by double-nozzle melt-spinning and subsequently annealed to produce a composite with a tailored nano/micro-crystalline structure. The overall magnetic behavior is characterized by butterfly-shaped high field hysteresis loops and positively biased low field ones. The main questions we wish to address here are whether the global magnetic behavior of the bilayer can be separated into the individual contributions of each layer and the magneto-coupling between them can be well understood. For that purpose, we performed first-order reversal curve analysis, which enabled us to distinctly identify two phases, of ultra-soft and semi-soft magnetic natures, whose mutual predominant interaction is the magnetostatic coupling. © *2015 AIP Publishing LLC*.
[http://dx.doi.org/10.1063/1.4932066]

The double-nozzle planar flow casting technique offers the possibility to obtain amorphous rapidly quenched bilayered ribbon composites. The simultaneous formation of two homogeneous layers with different composition and uniform thickness of tens of microns along the ribbon length makes possible combining unlike alloys with selected properties and unique overall behaviors. This possibility is particularly exciting in the case of magnetic materials in which the intimate coupling of alloys with different magnetic hardness may give rise to a variety of magnetization curves like constricted or biased hysteresis loops, along with vast technological application possibilities in magnetic devices and sensing elements.[1–4]

In this work, the magnetic behavior of a melt-spun $Fe_{73.5}Nb_3Si_{13.5}B_9Cu_1$ (FINEMET)/$Fe_{74.5}Nb_3Si_{13.5}B_9$ bilayer is studied. These alloys have been carefully chosen to join the required casting compatibility with different crystallization kinetics. On one hand, FINEMET is well known for its ability as precursor to produce, with the adequate thermal treatment, ultrasoft nanocrystalline systems.[5] Such annealing conditions lead in Cu-free $Fe_{74.5}Nb_3Si_{13.5}B_9$ to a microcrystalline structure with a harder, although still relatively soft, magnetic character. The resulting composite material is found to be an ultra-soft/semi-soft magnetic system presenting characteristic butterfly hysteresis loops, which are positively biased at low field.

Identifying the nature of mutual interactions between the layers as well as the interactions amongst the different magnetic phases within each layer is the key to understand the composite magnetic response. The traditional magnetic analysis based on the major magnetization curve provides global information which, in the case of multiphase systems, masks crucial individual properties and, perhaps more important, those interrelations, which rule the composite magnetic behavior. To overcome this limitation, the first-order reversal curve (FORC) method has been proposed, consisting of a full set of FORCs filling the hysteretic area of the major loop.[6–8] This technique involves an exigent measurement procedure and careful statistical data treatment,[9–11] which prove to be worthwhile when analyzing multiphase systems and magnetic interactions. Deciphering the information requires differential analysis combined with a physical model of the interacting constituents.[12,13]

In this work, the FORC technique applied to analyse the magnetism of the FINEMET/$Fe_{74.5}Nb_3Si_{13.5}B_9$ bilayer ribbon reveals with no ambiguity, as will be shown in the following lines, the magnetostatic nature of the dominant interaction coupling the layers.

The original bilayer ribbon was fabricated by rapid quenching from a single crucible using the double-nozzle technique.[14–16] The as-cast ribbon (6 mm wide and 50 μm thick) shows high quality surfaces and amorphous structure, evidenced from the absence of Bragg peaks in the x-ray diffraction patterns obtained on both sides. A 5 cm long sample of the ribbon was annealed in an inductive furnace under high vacuum to prevent surface oxidation. The annealing conditions (823 K for 1 h) were selected to get the optimal nanocrystalline state in the FINEMET layer.[17] Fig. 1(a) shows a cross-sectional image by scanning electron microscopy (SEM) where the sharp interface between the layers and their almost identical thickness can be appreciated. The sample was slightly tilted when the image was taken so, in its upper part, the roughness of the air surface of the ribbon can be appreciated. Different fracture mechanisms in both micro and nano-grained layers are the cause of the different fracture morphology, which is characterized by vertical features in the Cu-free layer. Transmission electron microscopy (TEM) shows different microstructures in both layers: Fig. 1(b) is a representative micrograph of the $Fe_{74.5}Nb_3Si_{13.5}B_9$ layer where large grains with an average size over 50 nm are seen; for its part, the FINEMET layer (see Fig. 1(c)) presents a homogeneous microstructure consisting

a)Electronic mail: rivas@uniovi.es

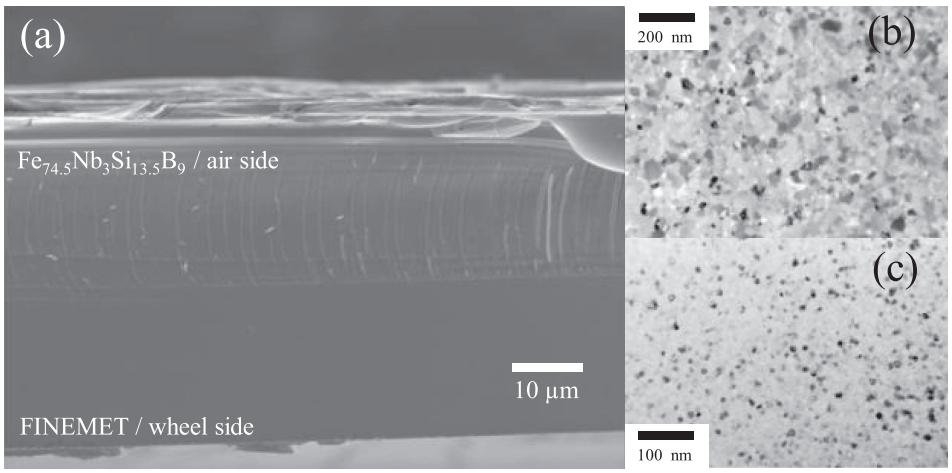

FIG. 1. (a) SEM image of a cross section of the annealed FINEMET/$Fe_{74.5}Nb_3Si_{13.5}B_9$ bilayer after annealing at 823 K for 1 h; (b) and (c) TEM micrographs corresponding to the microcrystallized $Fe_{74.5}Nb_3Si_{13.5}B_9$ and nanocrystallized FINEMET layers, respectively.

of nanocrystals with an average size ca. 10 nm surrounded by an amorphous matrix. The latter confirms the importance of Cu addition in order to promote the formation of ultrafine microstructure in FeSiB-based alloys.[18]

The FORCs were measured with an alternating adapted inductive magnetometer driven by a magnetic field, of maximum amplitude of 40 kA/m and 0.5 Hz, which was applied along the longitudinal direction of the ribbon. Each FORC is obtained by measuring the *M-H* curve between the return field H_r and the maximum applied field H_{max} (common to all the FORCs of the set) that should be quasi-saturating. A complete set of FORCs is measured for equi-spaced values of H_r from $-H_{max}$ to H_{max}.

The switching field distribution (SFD) corresponding to each FORC is then calculated as the derivative of the normalized magnetization m with respect to the applied field H

$$\mathrm{SFD}(H,H_r) = \left.\frac{\partial m}{\partial H}\right|_{H_r}. \quad (1)$$

The FORC diagram (FDiag) is the 2D graph display of the FORC distribution, traditionally defined as the mixed derivative of the magnetization

$$\rho(H,H_r) = -\frac{1}{2}\frac{\partial^2 m}{\partial H \partial H_r}. \quad (2)$$

Fig. 2 shows a set of 100 FORCs of the FINEMET/$Fe_{74.5}Nb_3Si_{13.5}B_9$ ribbon bilayer of this work and below the corresponding SFDs. Fig. 3 presents the calculated FDiag.

Fig. 2(a) shows a wasp-waisted major magnetization curve (light red colored), bespeaking a combination of two hysteresis loops with contrasting coercivities, one quasi-anhysteretical and other one magnetically harder, yet still relatively soft. Correspondingly, the major SFD curve in Fig. 2(b) presents two distinctly separated distributions and provides an estimation of the individual coercive fields from the position of the two peaks: $H_{c1} \simeq 0$ and $H_{c2} \simeq 2.8$ kA/m. The reason why these values have only the category of estimations is that the measured SFD (and the *M-H* curve) is obtained as a function of the applied field, which differs from the effective field that the material really senses due to the internal interactions. It is precisely on this difference where the ability of the FORC method to obtain information about the interaction resides.[19]

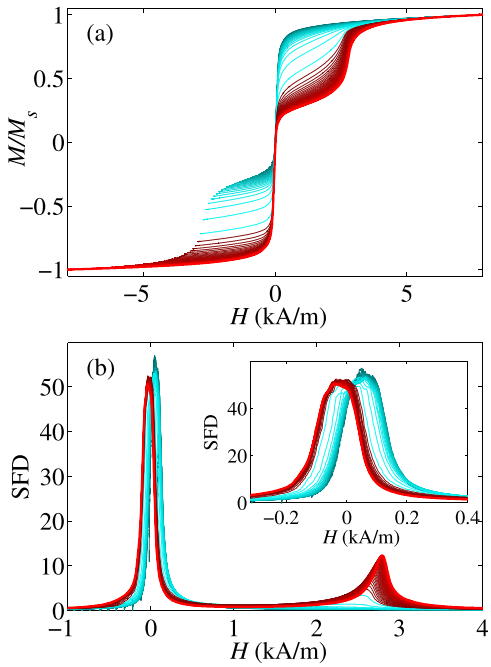

FIG. 2. (a) Set of 100 FORCs for the FINEMET/$Fe_{74.5}Nb_3Si_{13.5}B_9$ ribbon; the major magnetization curve is plotted in light red, the color goes from light to dark red when the return field H_r increases until the 50th FORC and then from light to dark blue. (b) SFDs associated with the above FORCs, following the same color criterion; inset: detail around the peak at $H = 0$.

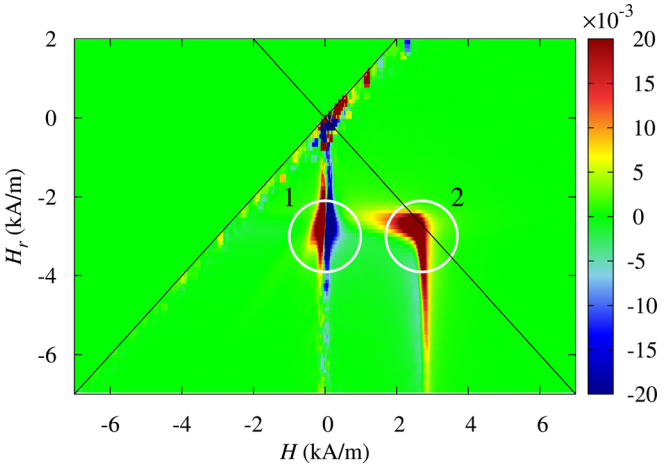

FIG. 3. FDiag obtained from the FORCs of Fig. 2. Regions 1 and 2, corresponding to ultra-soft and semi-soft phases, are highlighted.

It can be reasoned out that, taking as reference the intrinsic SFD (the distribution in terms of the effective field), the measured SFD is shifted to the right when the dominant interaction is positive (magnetizing interaction) and to the left when it is negative (demagnetizing interaction). Unfortunately, such effect cannot be directly observed as the intrinsic SFD is not obtainable so far, but the evolution of SFDs corresponding to successive FORCs can provide the clue.

The evolution of the successive FORCs relative to the major one can be interpreted on the basis of a mean interaction field kM, which produces a difference between the applied and the effective fields.[7,20] When a FORC is traced starting at $H_r > -H_{max}$, the difference between its initial magnetization and that of the major one is $\Delta M = M(H_r) - M(-H_{max}) > 0$. This difference, which remains along the curve until positive saturation is achieved, creates an extra interaction field $k\Delta M$. Such field shifts the minor SFD to the left of the major one if $k > 0$ or to the right if $k < 0$. In the FDiag, according to definition (2), this results in a pair of colored spots, which are blue-red (always blue color on the left) for $k > 0$ and red-blue for $k < 0$.[21]

FDiag of positive or negative interactions within one-phase systems[21–24] as well as for two positively coupled magnetic phases[25–27] are abundant in the literature. Nevertheless, round red-blue spots as that appearing in Fig. 3 (signaled as region 1) have never been published before.

A first look at the pattern of Fig. 3 reveals, consistently with Fig. 2, the existence of two well defined magnetic phases associated with the spots about H_{c1} and H_{c2}. Let us interpret this FDiag. The blue-red colored spot of region 2, corresponding to harder phase B, has a marked boomerang-shape, which indicates a strong positive interaction among the constituents of such phase, and whose vertical tail points to $H = H_{c2}$. The horizontal *head* of the boomerang appears in the interval $-3.2\,\text{kA/m} < H_r < -2.2\,\text{kA/m}$, for which the contribution of phase B to magnetization is clearly different at the beginning of each FORC, so producing large shifts of the SFDs and correspondingly, an intense fingerprint on the pattern. The fact that this spot appears for $H < -H_r$ is a clear evidence of positive interaction, which can undoubtedly be attributed to the exchange interaction among the relatively large crystallites. The average size of 50 nm seen in the micrograph of Fig. 1 is not sufficiently small, if compared to the exchange correlation length, to accommodate enough grains in the coupling volume to significantly reduce the effective anisotropy.

This explains the relatively hard behavior of phase B in contrast to phase A, whose ultra-soft character comes from the coupling of the very small nanocrystals (with sizes ca. 10 nm). The homogeneous size provides for the narrow SFD peak corresponding to phase A. In consequence, for $H_r < -3.2\,\text{kA/m}$, the FORCs start from a quasi-saturated state, hence no difference between the successive SFDs can be found, except around the peak $H = H_{c1}$ where an artifact with the shape of a vertical noisy strip is produced. This can be seen in the detail of the SFDs shown in the inset of Fig. 2(b) where all the curves in this interval of H_r mostly coincide within the experimental error responsible for the noise.

Just over this strip, in the range $-3.2\,\text{kA/m} < H_r < -2.2\,\text{kA/m}$, the SFD curves shift noticeably to the right for increasing H_r, indicating negative interaction which is translated to the FDiag as a round red-blue spot (region 1). It is not by chance that this spot coincides in the same return field range of region 2 as it is precisely the magnetostatic interaction of phase B upon phase A which produces it. For $H_r > -2.2\,\text{kA/m}$, phase B remains positively saturated, hence producing no difference between the SFD curves, which results in another meaningless noisy vertical strip above region 1.

Summing up, this red-blue structure and its position in the FDiag clearly signal a magnetostatic predominant interaction between the two magnetic layers. Consistently, one can expect that a sufficiently small field amplitude would switch the magnetization of the ultrasoft layer A while leaving phase B practically unaltered. Fig. 4 shows actually a minor loop which can be attributed mostly to layer A and which strongly depends on the magnetic history of layer B: when layer B is demagnetized (Fig. 4(a)), the resulting loop of layer A is centered at $H = 0$; when layer B has been previously oriented by a premagnetizing field strong enough to saturate it ($H_p \simeq 8\,\text{kA/m}$, according to Fig. 2), the minor

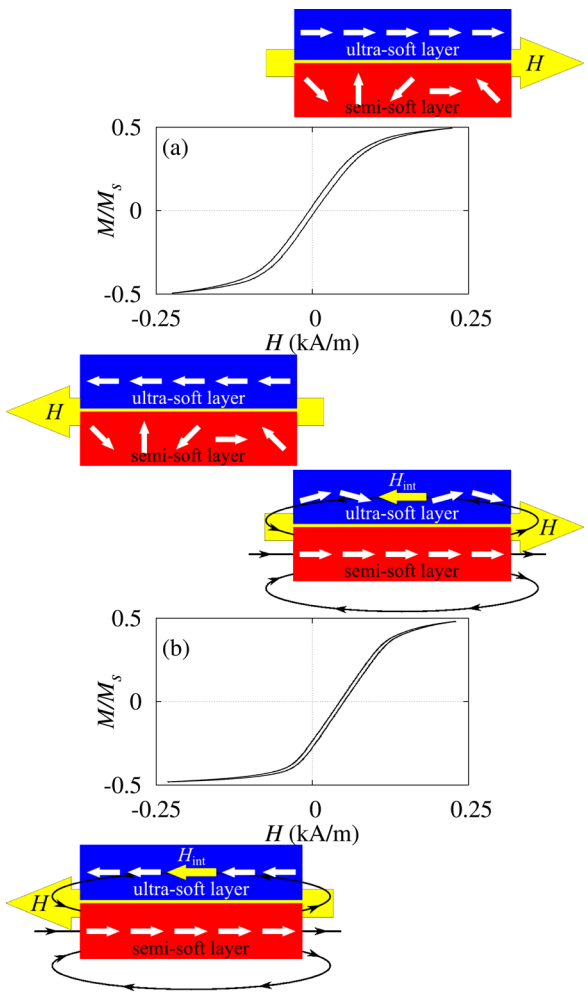

FIG. 4. Hysteresis loops of the ultrasoft layer A (a) when layer B is demagnetized, and (b) when layer B has been premagnetized with $H_p \simeq 8\,\text{kA/m}$. The schematic drawings illustrate the corresponding pseudo-saturation states: layer A (labelled ultra-soft layer) in blue color and layer B (semi-soft layer) in red color.

loop appears shifted to the right (Fig. 4(b)). The bias field value is a direct estimation of the average interaction field ($\langle H_{\text{int}} \rangle \simeq -50\,\text{A/m}$). As seen in the schematic drawings of Fig. 4(b), the magnetostatic field that layer B produces in layer A is negative no matter whether the applied field is positive or negative (as far as its amplitude does not affect appreciably the magnetization of layer B). This hinders the positive saturation while favors the negative one, leading to a global positive bias of the minor loop.

The relative influence of the two competing interlayer interactions, exchange and magnetostatic, is then clearly unveiled by this FORC analysis. Typically, in bi-phase devitrified systems, in which the harder phase is spread isotropically within the soft one, the magnetostatic field of the latter on the former cancels in overall. In contrast, the bilayer geometry is highly anisotropic, each layer producing a demagnetizing field on the other one. The exchange interaction, for its part, tends to keep the neighboring magnetic moments parallel and fades easily with distance, its effects affecting a few atomic layers far from crossing the width of the layer. The result is a negative magnetostatic predominant interaction responsible for the particular magnetic behavior of the global system unmistakably revealed by the FORC analysis.

This work was supported in part by the Spanish Ministry of Economy and Competitiveness under Project Nos. MAT2012-33405 and MAT2011-27573-C04-02, the Principality of Asturias under Project No. FC-15-GRUPIN14-037, IUTA/Gijón Council under Grant Nos. SV-14-GIJON-1-10, Slovak APVV-0492-11, Cex CFNT-MVEP, VEGA 2/0192/13, and PHYSNET ITMS 26110230097.

[1]O. Gutfleisch, M. A. Willard, E. Brück, C. H. Chen, S. G. Sankar, and J. P. Liu, Adv. Mater. **23**, 821 (2011).
[2]J. Liu, N. Scheerbaum, S. Weiß, and O. Gutfleisch, Appl. Phys. Lett. **95**, 152503 (2009).
[3]P. Álvarez, J. L. Sánchez Llamazares, P. Gorria, and J. A. Blanco, Appl. Phys. Lett. **99**, 232501 (2011).
[4]S. A. Wilson, R. P. J. Jourdain, Q. Zhang, R. A. Dorey, C. R. Bowen, M. Willander, Q. U. Wahab, S. M. Al-hilli, O. Nur, E. Quandt, C. Johansson, E. Pagounis, M. Kohl, J. Matovic, B. Samel, W. van der Wijngaart, E. W. H. Jager, D. Carlsson, Z. Djinovic, M. Wegener, C. Moldovan, R. Iosub, E. Abad, M. Wendlandt, C. Rusu, and K. Persson, Mater. Sci. Eng. R **56**, 1 (2007).
[5]Y. Yoshizawa, S. Oguma, and K. Yamauchi, J. Appl. Phys. **64**, 6044 (1988).
[6]A. P. Roberts, C. R. Pike, and K. L. Verosub, J. Geophys. Res. **105**, 28461, doi:10.1029/2000JB900326 (2000).
[7]F. Béron, D. Ménard, and A. Yelon, J. Appl. Phys. **103**, 07D908 (2008).
[8]C.-I. Dobrota and A. Stancu, J. Appl. Phys. **113**, 043928 (2013).
[9]C. R. Pike, A. P. Roberts, and K. L. Verosub, J. Appl. Phys. **85**, 6660 (1999).
[10]D. Heslop and A. R. Muxworthy, J. Magn. Magn. Mater. **288**, 155 (2005).
[11]F. Béron, G. Soares, and K. R. Pirota, Rev. Sci. Instrum. **82**, 063904 (2011).
[12]A. Stancu, C. Pike, L. Stoleriu, P. Postolache, and D. Cimpoesu, J. Appl. Phys. **93**, 6620 (2003).
[13]J. C. Martínez-García, M. Rivas, D. Lago-Cachón, and J. A. García, J. Alloys Compd. **615**, S276 (2014).
[14]P. Duhaj, P. Švec, E. Majková, V. Boháč, and I. Mat'ko, Mater. Sci. Eng. A **133**, 662 (1991).
[15]P. Švec, P. Švec, Sr., I. Mat'ko, I. Škorvánek, J. Kováč, D. Janičkovič, and G. Vlasák, Solid State Phenom. **172**, 953 (2011).
[16]A. Mitra, R. K. Roy, B. Mahato, A. K. Panda, G. Vlasák, D. Janičkovič, and P. Švec, J. Supercond. Nov. Magn. **24**, 611 (2011).
[17]P. Gorria, J. S. Garitaonandia, and J. M. Barandiarán, J. Phys. -Condens. Matter **8**, 5925 (1996).
[18]G. Herzer, Acta Mater. **61**, 718 (2013).
[19]M. Rivas, J. C. Martínez-García, and P. Gorria, "Visualizing decoupling in nanocrystalline alloys: A FORC-temperature analysis," J. Magn. Magn. Mater. (published online 2015).
[20]E. Della Torre, IEEE Trans. Acoust. Speech. **AU-14**, 86 (1966).
[21]J. C. Martínez-García, M. Rivas, D. Lago-Cachón, and J. A. García, J. Phys. D: Appl. Phys. **47**, 015001 (2014).
[22]R. Lavín, J. C. Denardin, J. Escrig, D. Altbir, A. Cortes, and H. Gomez, IEEE Trans. Magn. **44**, 2808 (2008).
[23]F. Béron, L. P. Carignan, D. Ménard, and A. Yelon, IEEE Trans. Magn. **44**, 2745 (2008).
[24]M. Almasi Kashi, A. Ramazani, and A. S. Esmaeily, IEEE Trans. Magn. **49**, 1167 (2013).
[25]N. Siadou, M. Androutsopoulos, I. Panagiotopoulos, L. Stoleriu, A. Stancu, T. Bakas, and V. Alexandrakis, J. Magn. Magn. Mater. **323**, 1671 (2011).
[26]D. Navas, J. Torrejon, F. Béron, C. Redondo, F. Batallan, and C. A. Cross, New J. Phys. **14**, 113001 (2012).
[27]F. Béron, L. A. S. de Oliveira, M. Knobel, and K. R. Pirota, J. Phys. D: Appl. Phys. **46**, 045003 (2013).